SECOND EUROPEAN CONFERENCE ON EARTHQUAKE ENGINEERING
AND SEISMOLOGY, ISTANBUL AUG. 25-29, 2014

ESTIMATING STRAIN PENETRATION FIXED-END ROTATIONS OF REINFORCED CONCRETE BEAM AND COLUMN MEMBERS

Panagiotis MERGOS[1] and Andreas KAPPOS[2]

ABSTRACT

Strain penetration of the longitudinal reinforcement of reinforced concrete (RC) beams and columns in the joints results in fixed-end rotations at the member ends. Several experimental studies have shown that fixed-end rotations caused by strain penetration contribute significantly (up to 50%) to the total displacement capacity of RC members. Hence, accurate determination of these fixed-end rotations at yielding and ultimate limit states becomes of primary importance when defining RC members structural response. Nevertheless, in existing literature, strain penetration fixed-end rotation is typically considered as secondary deformation mechanism and is examined always in combination with flexure. The purpose of this study is to present the theoretical background and the assumptions behind the relationships found in literature for determining strain penetration fixed-end rotations at yielding and ultimate. In addition, new simple relationships are proposed on the basis of realistic and mechanically-based assumptions. Comparisons between the existing and proposed relationships demonstrate the limitations of the existing approaches.

INTRODUCTION

Nowadays, performance based design gains ground on seismic design of RC structures. Basic prerequisite of reliable performance based design of RC structures is the trustworthy knowledge of individual members lateral displacement capacity at different performance levels.
In general, for RC members, lateral displacement capacity at yielding and ultimate may be considered as the sum of three individual components. The displacements developed by flexural and shear deformation mechanisms and the displacement due to strain penetration of the longitudinal reinforcement at the beam-column joints and/or footings. Estimation of the latter displacement component represents the main focus of the study presented herein.

Several experimental studies have shown that fixed-end rotations caused by strain penetration of longitudinal reinforcement in the joints contribute significantly (up to 50%) to the total displacement capacity of RC members (e.g. Ma et al. 1976, Saatcioglu and Ozcebe 1989, Lehman and Moehle 1998).

Various analytical methodologies have been developed so far for the determination of fixed-end rotations caused by strain penetration in the anchorage zone. These methodologies range from the most elaborate and accurate, which use the finite element or finite difference method (e.g. Viwathanatepa *et al.*1979, Ciampi *et al*. 1982, Filippou *et al*. 1983) to rather simplifying ones, yet accurate enough, which assume prescribed distributions of bond resistance along the anchorage length (e.g. Otani and Sozen 1972, Alsiwat and Saatcioglu 1992, Lowes and Altoontash 2003, Sezen and Setzler 2008, Mergos and Kappos 2012).

[1] Lecturer, City University, London UK, panagiotis.mergos.1@city.ac.uk
[2] Professor, City University, London UK, andreas.kappos.1@city.ac.uk

The main objective of this study is to propose new and simple closed-form relationships for calculating anchorage slip displacements at yielding and ultimate. The proposed relationships are based on appropriate mechanical background, which assures that all main parameters of anchorage slip effect are taken sufficiently into consideration. The new relationships are later used to evaluate widely adopted relationships in existing literature.

FIXED-END ROTATION AT YIELDING

If s denotes slippage of the tension reinforcement from its anchorage, fixed-end rotation θ_{slip} is given by Eq. (1), where x_c is the neutral axis depth and d is the member end section's effective depth.

$$\theta_{slip} = \frac{s}{d - x_c} \tag{1}$$

The most common assumption, when estimating anchorage slip fixed-end rotation at yielding, is that the bond stress τ_{be} is constant along the anchorage length L_{be} (Otani and Sozen 1972, Alsiwat and Saatcioglu 1992, Lowes and Altoontash 2003, Sezen and Setzler 2008, Fardis 2009). This assumption is generally effective but does not represent sufficiently the real phenomenon.

As shown in Fig. 1, when τ_{be} is assumed constant along the embedment length L_{be}, bar stress $\sigma_s(x)$ increases linearly from zero at the end of L_{be} to the bar yielding strength f_{yl} at the member end section. Since the bar remains in the elastic range, steel strains $\varepsilon_s(x)$ also increase linearly from zero to ε_y at the respective locations. Bar elongation at yielding s_y can now easily be calculated by integration:

$$s_y = \int_0^{L_{be}} \varepsilon_s(x)dx = \frac{1}{2} \cdot \varepsilon_y \cdot L_{be} \tag{2}$$

The embedment length L_{be} is determined by equilibrium for the bar with diameter d_{bl} as

$$\pi \cdot d_{bl} \cdot L_{be} \cdot \tau_{be} = \pi \cdot \frac{d_{bl}^{\,2}}{4} \cdot f_{yl} \rightarrow L_{be} = \frac{d_{bl} \cdot f_{yl}}{4 \cdot \tau_{be}} \rightarrow s_y = \frac{\varepsilon_y \cdot d_{bl} \cdot f_{yl}}{8 \cdot \tau_{be}} \tag{3}$$

Combining Eqs. (1), (2) and (3), the fixed-end rotation at yielding $\theta_{y,slip}$ is obtained as a function of the curvature at yielding $\varphi_y=\varepsilon_y/(d-x_c)$.

$$\theta_{y,slip} = \frac{s_y}{d - x_c} = \frac{1}{2} \cdot \frac{\varepsilon_y}{d - x_c} \cdot L_{be} = \varphi_y \cdot \frac{d_{bl} \cdot f_{yl}}{8 \cdot \tau_{be}} \tag{4}$$

One problem of the afore-described approach is the determination of the uniform bond stress τ_{be}. Fardis (2009) suggests that $\tau_{be} \approx \sqrt{f_c}$. This value is adopted by Fardis (2009) as the mean bond stress along L_{be} because it is about 50% or 40% of the maximum bond strength τ_{bu} of the local constitutive bond-slip law of unconfined or confined concrete, respectively, for "good" bond conditions according to CEB (1991) (see Fig. 2). The same value for τ_{be} is proposed by Lehman and Moehle (1998) and Sezen and Setzler (2008), who examined fixed-end rotations of RC columns subjected to cyclic loading. By setting $\tau_{be}=\sqrt{f_c}$, the following equation for $\theta_{y,slip}$ is obtained, which is the same as the one adopted in EC8-Part3.

$$\theta_{y,slip} = 0.13 \cdot \varphi_y \cdot \frac{d_{bl} \cdot f_{yl}}{\sqrt{f_c}} \tag{5}$$

Despite the convenience of the previous approach, it is not consistent with the actual bond-slip response. More particularly, it assumes constant bond stress along the anchorage length, while the slip increases quadratically from zero to the maximum value s_y at the beam-column end section. This is not consistent with the local bond-slip constitutive law presented in Fig. 2.

To overcome this limitation, a new and simple procedure is proposed herein for evaluating s_y. The method assumes that the bond stress is a general power function of the distance x from the anchorage point of zero stress, strain and slip (see Fig. 3). Hence, it is assumed:

$$\tau_b(x) = b \cdot x^c \tag{6}$$

It is worth noting that Eq. (6) at x=0 yields $\tau_b(x)$=0, which is in accordance with the boundary condition $s(x)$=0 at x=0 and the local constitutive bond-slip law shown in Fig. 2.

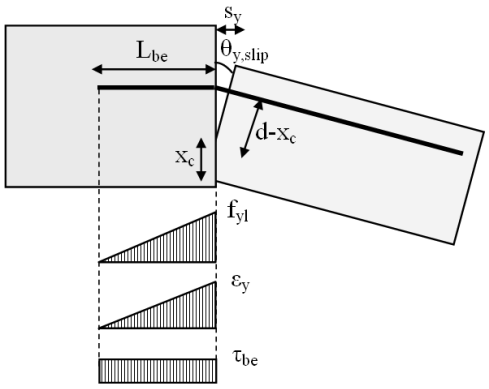

Figure 1: Determination of fixed-end rotation at yielding by assuming uniform bond stress distribution

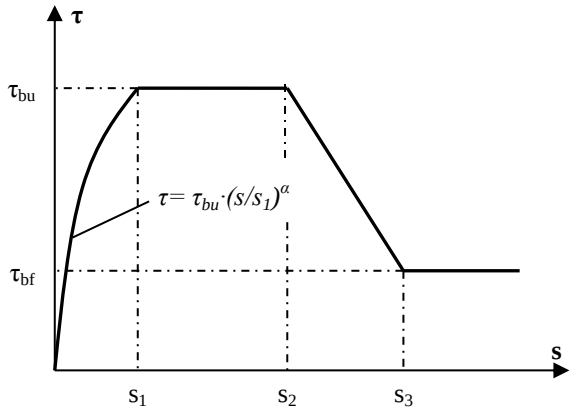

Figure 2: Local constitutive bond-slip law (adopted by CEB (1991))

Parameters b and c are considered unknown and will be determined in the following by satisfying local bond-slip law at $x=L_{be}$ and at an arbitrary anchorage point P at distance $x=x_P=L_{be}/m$, where $m>1$ (see Fig. 3). Thus, no additional assumptions are induced for the calculation of b and c.

The proposed method assumes that all points along L_{be} remain in the ascending branch of the local bond-slip law. Hence, at the end of the calculations, the following relationship should hold: $s_y < s_1$ (see Fig. 2).

Application of Eq. (6) to the two points mentioned above, gives:

$$\left.\begin{aligned}\tau_{by} &= b \cdot L_{be}{}^{c} \\ \tau_{bP} &= b \cdot \left(\frac{L_{be}}{m}\right)^{c}\end{aligned}\right\} \rightarrow \frac{\tau_{by}}{\tau_{bP}} = m^{c} \tag{7}$$

By equilibrium of an infinitesimal anchorage length dx and the boundary condition (x=0 → σ_s=0), one obtains:

$$\frac{d\sigma_s}{dx} = \frac{4}{d_{bl}} \cdot \tau_b(x) \rightarrow \frac{d\sigma_s}{dx} = \frac{4}{d_{bl}} \cdot b \cdot x^{c} \rightarrow \sigma_s(x) = \frac{4b}{d_{bl}} \cdot \int x^{c} dx \rightarrow \sigma_s(x) = \frac{4}{d_{bl}} \cdot \frac{b}{c+1} \cdot x^{c+1} \tag{8}$$

For x=L_{be}, it is assumed that the steel bar is at the point of yield or else σ_s=f_{yl}. Solving for L_{be} and using Eq. (7), one obtains:

$$f_{yl} = \frac{4}{d_{bl}} \cdot \frac{b}{c+1} \cdot L_{be}{}^{c+1} = \frac{4}{d_{bl}} \cdot \frac{\tau_{by}}{c+1} \cdot L_{be} \rightarrow L_{be} = \frac{f_{yl} \cdot d_{bl} \cdot (c+1)}{4\tau_{by}} \tag{9}$$

Furthermore, since the reinforcement bar remains in the elastic region, it holds:

$$\varepsilon_s(x) = \frac{\sigma_s(x)}{E} = \frac{4}{E \cdot d_{bl}} \cdot \frac{b}{c+1} \cdot x^{c+1} \tag{10}$$

Where E is the elastic modulus of steel. By ignoring the strain of concrete and by applying the boundary condition $s(x)=0$ at $x=0$, slip $s(x)$ at distance x becomes:

$$s(x) = \int \varepsilon_s(x) dx = \frac{4}{E \cdot d_{bl}} \cdot \frac{b}{c+1} \cdot \int x^{c+1} dx = \frac{4}{E \cdot d_{bl}} \cdot \frac{b}{(c+1)\cdot(c+2)} \cdot x^{c+2} \tag{11}$$

At x=L_{be} and at x=x_P, by using Eq. (11), anchorage slips s_y and s_p respectively are related as:

$$\left.\begin{aligned}s_y &= \frac{4}{E \cdot d_{bl}} \cdot \frac{b}{(c+1)\cdot(c+2)} \cdot L_{be}{}^{c+2} \\ s_P &= \frac{4}{E \cdot d_{bl}} \cdot \frac{b}{(c+1)\cdot(c+2)} \cdot \left(\frac{L_{be}}{m}\right)^{c+2}\end{aligned}\right\} \rightarrow \frac{s_y}{s_P} = m^{c+2} \tag{12}$$

Moreover, by considering the relationship of the bond-slip constitutive law ascending branch shown in Fig. 2 and Eq. (7), it is obtained:

$$\left.\begin{aligned}\tau_{by} &= \left(\frac{s_y}{s_1}\right)^{a} \cdot \tau_{bu} \\ \tau_{bP} &= \left(\frac{s_P}{s_1}\right)^{a} \cdot \tau_{bu}\end{aligned}\right\} \rightarrow \frac{\tau_{by}}{\tau_{bP}} = \left(\frac{s_y}{s_P}\right)^{\alpha} \rightarrow \left(\frac{s_y}{s_P}\right)^{\alpha} = m^{c} \tag{13}$$

Combining Eqs. (12) and (13) and since m is an arbitrary number, it gets:

$$\left(\frac{s_y}{s_P}\right)^{\alpha} = m^{c} \rightarrow \left(m^{c+2}\right)^{\alpha} = m^{c} \rightarrow a \cdot (c+2) = c \rightarrow c = \frac{2\alpha}{1-a} \tag{14}$$

Slip s_y can now be determined by applying Eq. (11) together with Eq. (9):

$$s_y = \frac{4}{E \cdot d_{bl}} \cdot \frac{b}{(c+1)\cdot(c+2)} \cdot L_{be}^{\,c+2} = \frac{f_{yl} \cdot L_{be}}{E \cdot (c+2)} = \frac{\varepsilon_y \cdot L_{be}}{(c+2)} \tag{15}$$

By further substitution of L_{be} from Eq. (9) and the use of the local bond-slip constitutive law, it is obtained:

$$s_y = \frac{\varepsilon_y \cdot f_{yl} \cdot (c+1) \cdot d_{bl}}{4(c+2) \cdot \tau_{by}} = \frac{\varepsilon_y \cdot f_{yl} \cdot (c+1) \cdot d_{bl}}{4(c+2) \cdot \left(\frac{s_y}{s_1}\right)^a \cdot \tau_{bu}} \rightarrow \tag{16}$$

Finally, by substituting c from Eq. (14) and solving for s_y/s_1, it becomes:

$$\frac{s_y}{s_1} = \sqrt[1+a]{\frac{(1+a)\cdot\varepsilon_y \cdot f_{yl} \cdot d_{bl}}{8 \cdot s_1 \cdot \tau_{bu}}} \tag{17}$$

It is important to note that Eq. (17) provides a closed-form solution to the calculation of s_y from the steel properties and the local bond-slip constitutive law parameters. The proposed methodology takes into account the variation of bond stress along the anchorage length, while the average bond stress method adopted in EC8 violates the local bond-slip constitutive law.

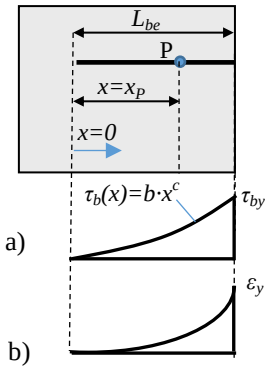

Figure 3: Proposed solution methodology: a) bond stress distribution and b) steel strain distribution along L_{be}

One of the advantages of the proposed methodology is the fact that it calculates s_y as a function of local constitutive bond-slip law parameters that have already been calibrated for different bond conditions and levels of confinement. Fig. 4a compares s_y predictions for different bar diameters derived by the uniform bond stress assumption $\tau_{be}=\sqrt{f_c}$ (i.e. EC8-Part 3 approach) and the proposed methodology for "Confined" or "Unconfined" concrete and "Good" or "Poor" bond conditions in accordance with the definitions proposed in CEB (1991). In particular, four discrete combinations are examined and named by a first letter corresponding to the level of confinement followed by a second letter indicating bond conditions (i.e. U/G means "Unconfined" concrete in "Good" bond conditions). CEB (1991) constitutive bond-slip law parameters are assigned for each of the combinations. Concrete compressive strength is assumed equal to f_c=25MPa and steel yielding strength f_{yl}=500MPa.

It can be seen that s_y predictions differ significantly for the different combinations of confinement and bond conditions. The highest s_y are predicted for the confined concrete in poor bond conditions and the lowest for unconfined concrete in good bond conditions. This happens because according to CEB (1991) constitutive model, the former combination demonstrates the most and the latter the least stiff ascending branches.

It is also interesting to compare EC8-Part 3 predictions with the predictions of the proposed methodology for confined concrete in "good" bond conditions. It is recalled that the value τ_{be} adopted in EC8-Part 3 is taken as 50% or 40% of the maximum bond strength τ_{bu} of the local constitutive bond-slip law of unconfined or confined concrete, respectively, for "good" bond conditions according to CEB (1991). It can be seen that the two solutions tend to converge for small bar diameters, but they deviate significantly for large bar diameters. This observation drives to the conclusion that no unique uniform τ_{be} can be assumed for all bar diameters, as assumed in EC8-Part 3.

It is important to note that the proposed solution can be readily applied to the calculation of anchorage slip when the steel strain at the beam-column end section ε_{so} is smaller than ε_y. This is achieved by setting in Eq. (17) ε_{so} instead of ε_y and corresponding stress $\sigma_{so} = E \cdot \varepsilon_{so}$ instead of f_{yl}.

Fig. 4b compares anchorage slip calculated by the EC8-Part 3 and proposed approaches for the same material properties as above and bar diameter d_{bl}=8mm. As it can be seen in Fig. 4b, s_y predictions of the two methodologies coincide for this bar diameter size. However, further comparison reveals that EC8-Part 3 approach may considerably underestimate anchorage slip at low steel stresses. This is because the constant bond stress value $\tau_{be}=\sqrt{f_c}$ assumed by EC8-Part 3 corresponds only to yielding of the longitudinal reinforcement. For lower steel stresses, lower slips and bond stresses are expected. Hence, EC8-Part 3 approach may overestimate bond and underestimate slip of the anchorage.

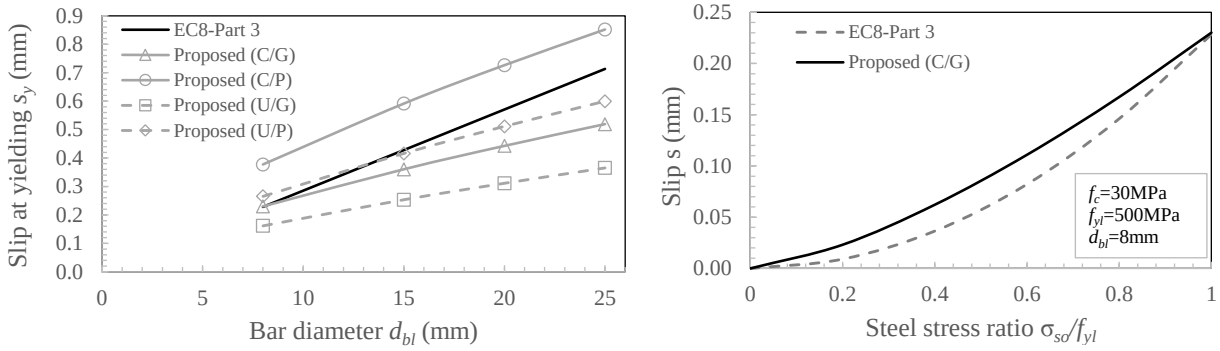

Figure 4: Variation of a) s_y with d_{bl}; b) s with f_{so}/f_{yl} according to EC8-Part3 and the proposed methodology

FIXED-END ROTATION AT ULTIMATE

For the calculation of anchorage slip fixed-end rotation at ultimate $\theta_{u,slip}$ the additional 'plastic' fixed-end rotation arising from the inelastic part $L_{bp,u}$ of the anchorage $\theta_{pu,slip}$ should be added to $\theta_{y,slip}$. Typically, $\theta_{pu,slip}$ is significantly higher than $\theta_{y,slip}$ due to the large strains and the reduced bond capacity developed in the inelastic part of the anchorage. To calculate accurately $\theta_{pu,slip}$ elaborate analytical methodologies are generally required like the ones mentioned in the introduction of this study.

In addition to these methodologies, a number of researchers have made various simplifying assumptions in order to provide approximate estimates of $\theta_{pu,slip}$. The most widely adopted approach for calculating $\theta_{pu,slip}$ at onset of flexural failure is the equivalent plastic hinge length approach (Priestley *et al*. 2007, Fardis 2009). According to this approach, $\theta_{pu,slip}$ can be determined by the following equation, where $L_{sp,u}$ is the strain penetration length at flexural failure:

$$\vartheta_{pu,slip} = \left(\varphi_u - \varphi_y\right) \cdot L_{sp,u} \tag{18}$$

Different empirical relationships have been proposed in the literature for the calculation of $L_{sp,u}$. Priestley et al. (2007) propose that $L_{sp,u}$ is calculated by the following equation (f_{yl} in MPa).

$$L_{sp,u} = 0.022 \cdot d_{bl} \cdot f_{yl} \tag{19}$$

Depending on the way the curvature of the RC member end section at flexural failure φ_u is calculated, EC8-Part 3 proposes two different equations for the determination of $L_{sp,u}$ (f_{yl}, f_c in MPa).

$$L_{sp,u} = 0.24 \cdot \frac{d_{bl} \cdot f_{yl}}{\sqrt{f_c}} \tag{20}$$

$$L_{sp,u} = 0.11 \cdot \frac{d_{bl} \cdot f_{yl}}{\sqrt{f_c}} \tag{21}$$

At this point, it is important to mention that the actual value of $L_{sp,u}$ cannot be treated as independent of the assumptions made for the calculation of φ_u in moment-curvature analysis. These assumptions concern the constitutive models for confined and unconfined concrete, the constitutive model for reinforcing steel, the determination of the ultimate concrete strain at failure ε_{cu} and the steel strain at failure ε_{su}. A thorough description of the assumptions made for the determination of φ_u in the three different equations of $L_{sp,u}$ (Eqs. 19 to 21) can be found in Fardis (2009).

The previous observation represents one of the main drawbacks of Eqs. (19)-(21). Since, a constant value of $L_{sp,u}$ is assumed this has to be calibrated separately for the various assumptions (strain limits) corresponding to φ_u. Furthermore, the relationships for $L_{sp,u}$ can be used only for calculating $\theta_{pu,slip}$ at flexural failure and not for the determination of $\theta_{p,slip}$ at limit states prior to failure.

In the following, a more general approach for determining L_{sp} (i.e. strain penetration length at all limit states prior to flexural failure) will be developed. The methodology is based on the assumption of uniform bond stress distribution inside L_{bp} (Fig. 5). The same assumption has been made by several researchers (e.g. Alsiwat and Saatcioglu 1992, Lehman and Moehle 1998, Lowes and Altoontash 2003, Sezen and Setzler 2008, Mergos and Kappos 2012) with good correlation of the experimental measurements and the analytical calculations. However, these research efforts aimed at calculating directly $\theta_{p,slip}$ and not L_{sp}. In this study, an analytical relationship for L_{sp} is targeted that will drive to the calculation of $\theta_{p,slip}$ directly from the moment-curvature analysis of the member end section and without further additional considerations.

An important issue when calculating $\theta_{p,slip}$ is the assumption regarding the reinforcing steel strain-hardening constitutive law. The vast majority of analytical models (e.g. Alsiwat and Saatcioglu 1992, Lehman and Moehle 1998, Lowes and Altoontash 2003) assume linear hardening constitutive law, mostly for simplicity reasons. Nevertheless, a previous analytical study by Mergos and Kappos (2012) has shown that the nonlinearity of the strain-hardening material law plays a significant role in the determination of $\theta_{p,slip}$. Hence, in the following, closed form relationships will be derived for both linear and nonlinear strain hardening laws of reinforcing steel.

Linear strain-hardening law

Figure 5 illustrates bond stress, steel stress and steel strain distribution along L_{bp}, where plastic reinforcement slip s_p and the corresponding fixed-end rotation $\theta_{p,slip}$ are developed. When linear strain-hardening law is assumed, then steel stress after yielding σ_s is given by Eq. (22) as a function of the respective steel stress ε_s and the steel stress f_{su} and strain ε_{su} at maximum strength. For simplicity reasons, the yield plateau region (which, in any case is an idealization of the observed behavior) is not taken into consideration. This is not expected to influence significantly the results since the steel stress remains constant in this region and no additional strain penetration is developed.

$$\sigma_s = f_{yl} + \left(f_{su} - f_{yl} \right) \cdot \frac{\left(\varepsilon_s - \varepsilon_y \right)}{\left(\varepsilon_{su} - \varepsilon_y \right)} \tag{22}$$

The inelastic anchorage length L_{bp} is determined by equilibrium and by using Eq. (22). In Eq. (23), σ_{so} and ε_{so} are the steel stress and strain at the anchorage loaded end (Fig. 5).

$$\pi \cdot d_b \cdot L_{bp} \cdot \tau_{bp} = \pi \cdot \frac{d_{bl}^{\,2}}{4} \cdot \left(\sigma_{so} - f_{yl}\right) \rightarrow L_{bp} = \frac{d_{bl} \cdot \left(\sigma_{so} - f_{yl}\right)}{4 \cdot \tau_{bp}} = \frac{d_{bl} \cdot \left(\varepsilon_{so} - \varepsilon_y\right)}{4 \cdot \tau_{bp}} \cdot \frac{\left(f_{su} - f_{yl}\right)}{\left(\varepsilon_{su} - \varepsilon_y\right)} \quad (23)$$

For linear strain distribution, post-yield anchorage slip s_p is easily calculated as

$$s_p = \int_0^{L_{bp}} \varepsilon_s(x)dx = \frac{\varepsilon_{so} + \varepsilon_y}{2} \cdot L_{bp} = \frac{d_{bl} \cdot \left(\varepsilon_{so} - \varepsilon_y\right) \cdot \left(\varepsilon_{so} + \varepsilon_y\right)}{8 \cdot \tau_{bp}} \cdot \frac{\left(f_{su} - f_{yl}\right)}{\left(\varepsilon_{su} - \varepsilon_y\right)} \quad (24)$$

The respective fixed-end rotation is given by the following equation, which makes the common assumption that the neutral axis depth remains approximately constant after yielding of the longitudinal reinforcement. In this equation, φ_o is the curvature of the critical end section of the RC member.

$$\vartheta_{p,slip} = \frac{s_p}{d - x_c} \approx \frac{d_{bl} \cdot \left(\varphi_o - \varphi_y\right) \cdot \left(\varepsilon_{so} + \varepsilon_y\right)}{8 \cdot \tau_{bp}} \cdot \frac{\left(f_{su} - f_{yl}\right)}{\left(\varepsilon_{su} - \varepsilon_y\right)} \quad (25)$$

The strain penetration length L_{sp} can now be calculated as:

$$L_{sp} = \frac{\vartheta_{p,slip}}{\varphi_p} = \frac{\vartheta_{p,slip}}{\left(\varphi_o - \varphi_y\right)} = \frac{d_{bl} \cdot \left(\varepsilon_{so} + \varepsilon_y\right)}{8 \cdot \tau_{bp}} \cdot \frac{\left(f_{su} - f_{yl}\right)}{\left(\varepsilon_{su} - \varepsilon_y\right)} = \frac{d_{bl} \cdot \left(\varepsilon_{so} - \varepsilon_y + 2\varepsilon_y\right)}{8 \cdot \tau_{bp}} \cdot \frac{\left(f_{su} - f_{yl}\right)}{\left(\varepsilon_{su} - \varepsilon_y\right)} \quad (26)$$

It is emphasized that L_{sp} of Eq. (26) is valid for all curvatures after φ_y and it is not restricted only to φ_u. The equation above can be also written in the following form:

$$L_{sp} \approx \frac{\left(f_{su} - f_{yl}\right) \cdot d_{bl}}{8 \cdot \tau_{bp}} \cdot \left(\varepsilon_{no} + 2\varepsilon_y\right) \quad (27)$$

In Eq. (27), ε_{no} is the normalized post-yield strain ratio $\varepsilon_{no}=(\varepsilon_{so}-\varepsilon_y)/(\varepsilon_{su}-\varepsilon_y)$. Clearly, in the post-yield range, ε_{no} ranges from zero to unity. According to the same equation, L_{sp} increases linearly with the normalized post-yield strain ratio ε_{no}. Eq. (27) can also be written as:

$$L_{sp} = \frac{\left(f_{su} - f_{yl}\right) \cdot d_{bl}}{8 \cdot \tau_{bp}} \cdot \varepsilon_{no} + \frac{\left(f_{su} - f_{yl}\right) \cdot d_{bl}}{4 \cdot \tau_{bp}} \cdot \frac{\varepsilon_y}{\varepsilon_{su} - \varepsilon_y} = \frac{\left(\sigma_{so} - f_{yl}\right) \cdot d_{bl}}{8 \cdot \tau_{bp}} + \frac{\left(f_{su} - f_{yl}\right) \cdot d_{bl}}{4 \cdot \tau_{bp}} \cdot \frac{\varepsilon_y}{\varepsilon_{su} - \varepsilon_y} \quad (28)$$

The second term of Eq. (28) can generally be neglected because $\varepsilon_y << \varepsilon_{su}$. In this case, L_{sp} takes the simple form of Eq. (29):

$$L_{sp} = \frac{\left(\sigma_{so} - f_{yl}\right) \cdot d_{bl}}{8 \cdot \tau_{bp}} \quad (29)$$

The post-yield fixed-end rotation $\theta_{p,slip}$ corresponding to arbitrary post-yield curvature φ_o and steel strain σ_{so} of the RC member end-section can now be calculated by the simple equation:

$$\theta_{p,slip} = \left(\varphi_o - \varphi_y\right) \cdot L_{sp} = \left(\varphi_o - \varphi_y\right) \cdot \frac{\left(\sigma_{so} - f_{yl}\right) \cdot d_{bl}}{8 \cdot \tau_{bp}} \quad (30)$$

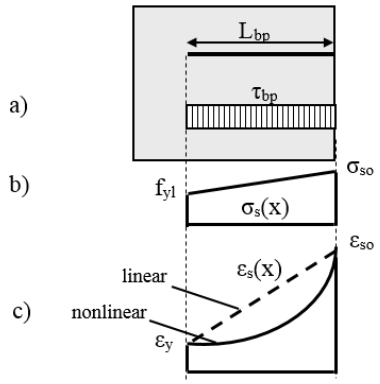

Figure 5: Inelastic part of the anchorage: a) bond stress distribution; b) steel stress distribution; c) steel strain distribution.

Nonlinear strain-hardening law

Nonlinearity of the strain-hardening law increases considerably the level of difficulty of the analytical derivation of post-yield anchorage slip s_p. Hence, it is generally more appropriate to calculate s_p by numerical integration of the steel strains inside L_{bp}.

In this study, the nonlinear strain-hardening law suggested by Priestley *et al*. (2007) is examined. This is given by the following relationship:

$$\sigma_s = f_{su} - \left(f_{su} - f_{yl} \right) \cdot \left(\frac{\varepsilon_{su} - \varepsilon_s}{\varepsilon_{su} - \varepsilon_y} \right)^2 \tag{31}$$

The steel stress $\sigma_s(x)$ at a distance x from the loaded end of the anchorage is determined by equilibrium

$$\sigma_s(x) = \sigma_{so} - \frac{4\tau_{bp}}{d_{bl}} \cdot x \tag{32}$$

Hence, the respective steel strain can be calculated by combining Eq. (31) and Eq. (32)

$$\varepsilon_s(x) = \varepsilon_{su} - \left(\varepsilon_{su} - \varepsilon_y \right) \cdot \sqrt{\frac{f_{su} - \sigma_s(x)}{f_{su} - f_{yl}}} = \varepsilon_{su} - \left(\varepsilon_{su} - \varepsilon_y \right) \cdot \sqrt{\frac{f_{su} - \sigma_{so} + 4\tau_{bp} \cdot x / d_{bl}}{f_{su} - f_{yl}}} \tag{33}$$

The anchorage slip s_p developed in L_{bp} is calculated by strain integration along this length.

$$s_p = \int_0^{L_{bp}} \varepsilon_s(x) dx = \int_0^{L_{bp}} \left(\varepsilon_{su} - \left(\varepsilon_{su} - \varepsilon_y \right) \cdot \sqrt{\frac{f_{su} - \sigma_{so} + 4\tau_{bp} \cdot x / d_{bl}}{f_{su} - f_{yl}}} \right) dx \tag{34}$$

It is recalled that L_{bp} is given by the general Eq. (35)

$$\pi \cdot d_b \cdot L_{bp} \cdot \tau_{bp} = \pi \cdot \frac{d_{bl}^2}{4} \cdot \left(\sigma_{so} - f_{yl} \right) \rightarrow L_{bp} = \frac{d_{bl} \cdot \left(\sigma_{so} - f_{yl} \right)}{4 \cdot \tau_{bp}} \tag{35}$$

Now, the equivalent plastic hinge length for anchorage slip L_{sp} can be determined by the following equation:

$$L_{sp} = \frac{\vartheta_{p,slip}}{\varphi_p} = \frac{s_p}{\left(\varphi_o - \varphi_y\right)\cdot\left(d - x_c\right)} \approx \frac{s_p}{\left(\varepsilon_{so} - \varepsilon_y\right)} \tag{36}$$

Eqs. (34)-(36) were solved numerically for different reinforcing steel parameters and it was found that the numerical solution can always be written in the following general form, where $\lambda(\varepsilon_{no})$ is a function of $\varepsilon_{no}=(\varepsilon_{so}-\varepsilon_y)/(\varepsilon_{su}-\varepsilon_y)$.

$$L_{sp} = \frac{\left(f_{su} - f_{yl}\right)\cdot d_{bl}}{8\cdot\tau_{bp}}\cdot\lambda\left(\varepsilon_{no}\right) \tag{37}$$

Fig. (6a) presents variation of $\lambda(\varepsilon_{no})$ with ε_{no}. It can be seen that $\lambda(\varepsilon_{no})$ increases initially nonlinearly with ε_{no} and then tends to stabilize. In fact, when ε_{no} approaches unity, $\lambda(\varepsilon_{no})$ slightly decreases, but this can be neglected for practical applications. The maximum value of $\lambda(\varepsilon_{no})$ is approximately ¾.

More interestingly, Fig. (6b) shows the variation of λ with the normalized ratio $\sigma_{no}=(\sigma_{so}-f_{yl})/(f_{su}-f_{yl})$. In this figure, it can be seen that $\lambda(\sigma_{no})$ increases almost linearly from zero to ¾ as σ_{no} increases from zero to unity. This observation drives to the conclusion that for practical applications, Eq. (37) can be written as:

$$L_{sp} \approx \frac{3}{4}\cdot\frac{\left(\sigma_{so} - f_{yl}\right)\cdot d_{bl}}{8\cdot\tau_{bp}} \tag{38}$$

Comparing Eqs. (29) and (38), it can be observed that they can both be written in the following general form:

$$L_{sp} = \frac{\left(\sigma_{so} - f_{yl}\right)\cdot d_{bl}}{8\cdot\tau_{bp}}\cdot\mu \tag{39}$$

where μ is a factor that accounts for the constitutive strain hardening law of the steel (i.e. μ=1 for linear hardening law and μ=3/4 for quadratic hardening law). It is worth noting that for the nonlinear hardening law it is $\mu<1$. This is due to the fact that for the same σ_{no} strains along L_{bp} are generally lower than the ones corresponding to linear hardening law as it is evident in Fig. 5.

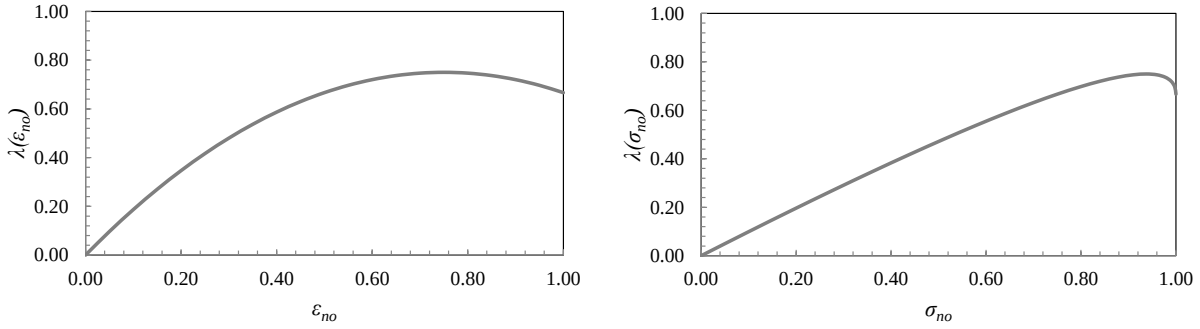

Figure 6: Variation of λ with a) ε_{no}; b) σ_{no}

Eq. (39) leads to the conclusion that L_{sp} cannot exceed the following maximum value:

$$L_{sp,\max} = \frac{\left(f_{su} - f_{yl}\right)\cdot d_{bl}}{8\cdot\tau_{bp}}\cdot\mu \tag{40}$$

A crucial issue when employing Eqs. (35) and (36) is the value of the average bond stress τ_{bp} along L_{bp}. Lehman and Moehle (1998) based on experimental measurements of well confined bridge piers subjected to cyclic loading suggest that $\tau_{bp}=0.5\sqrt{f_c}$. This effectively means that for less confined columns in "poor" bond conditions smaller values should be assumed. Alsiwat and Saatcioglu (1992) propose that τ_{bp} is taken equal to the frictional bond strength τ_{bf} of the constitutive bond-slip law shown in Fig. 2. Depending on the level of confinement and the quality of bond conditions (i.e. "good" or "poor") and according to CEB (1991) τ_{bf} ranges between $0.15\sqrt{f_c}$ and $\sqrt{f_c}$. It is also important that the value of τ_{bp} takes into consideration the degradation of bond strength capacity with cyclic loading.

As described above, it is generally suggested that τ_{bp} is taken as $\tau_{bp}=\psi\cdot\sqrt{f_c}$ where ψ is a constant parameter (e.g. ψ=0.5 according to Lehman and Moehle 1998).

By substituting τ_{bp} in Eq. (39), L_{sp} takes the following general form:

$$L_{sp}=\frac{\left(\sigma_{so}-f_{yl}\right)\cdot d_{bl}}{8\cdot\psi\cdot\sqrt{f_c}}\cdot\mu=\left\lceil\frac{\left(\sigma_{so}/f_{yl}-1\right)}{8\cdot\psi}\cdot\mu\right\rceil\cdot\frac{f_{yl}\cdot d_{bl}}{\sqrt{f_c}} \tag{41}$$

The strain penetration length at flexural failure $L_{sp,u}$ can be determined by direct substitution as:

$$L_{sp,u}=\left\lceil\frac{\left(\sigma_{so,u}/f_{yl}-1\right)}{8\cdot\psi}\cdot\mu\right\rceil\cdot\frac{f_{yl}\cdot d_{bl}}{\sqrt{f_c}} \tag{42}$$

The form of Eq. (42) can be considered as a generalization of the Eqs. (19-21) that are widely adopted in the calculation of $L_{sp,u}$ (Priestley *et al*. 2007, Fardis 2009). The general form of all equations is the following, where κ factor is given by Eq. (44).

$$L_{sp,u}=\kappa\cdot\frac{f_{yl}\cdot d_{bl}}{\sqrt{f_c}} \tag{43}$$

$$\kappa=\frac{\left(\sigma_{so,u}/f_{yl}-1\right)}{8\cdot\psi}\cdot\mu \tag{44}$$

Eqs. (43) and (44) are illustrative because they reveal the influence of various parameters on $L_{sp,u}$. More particularly, it is shown that $L_{sp,u}$ increases with f_{yl} and d_{bl} and decreases with $\sqrt{f_c}$. These observations are in accordance with models in existing literature. In addition, Eq. (44) shows that $L_{sp,u}$ depends on the steel stress at failure, the strain-hardening constitutive law and the general bond conditions (i.e. level of confinement and position of the reinforcement). The latter parameters are not taken explicitly into consideration in Eqs. (19-21).

Figure 7 illustrates the range of κ values for typical values of ψ ($0.1\leq\psi\leq1$) and $\sigma_{so,u}/f_{yl}$ ($1.1\leq\sigma_{so,u}/f_{yl}\leq1.5$) for nonlinear hardening constitutive law (i.e. μ=3/4). It can be seen that κ varies from 0.01 to 0.47. It is recalled that according to EC8-Part 3 κ is either 0.11 or 0.24. Hence, it is obvious that EC8-Part 3 may lead to serious underestimation or overestimation of $L_{sp,u}$ and consequently $\theta_{pu,slip}$.

In Eq. (44), $\sigma_{so,u}$ is the steel stress corresponding to onset of flexural failure of the RC member end-section. Usage of $\sigma_{so,u}$, instead of f_{su}, is strongly recommended for non-ductile RC members that can fail in flexure at steel stress levels significantly lower than f_{su}. This depends also on the type of the reinforcing steel strain-hardening law. For linear hardening law, for example, it is still unlikely that $\sigma_{so,u}$ will reach f_{su} even for well confined members. In addition to the above, it should be clarified that $L_{sp,u}$ should not be used for the determination of $\theta_{p,slip}$ as it will lead to overestimation of the post-yield fixed-end rotations. Instead, the value of L_{sp} corresponding to the examined curvature of the member end-section should be applied. L_{sp} varies from 0 at yielding to $L_{sp,u}$ at onset of flexural failure.

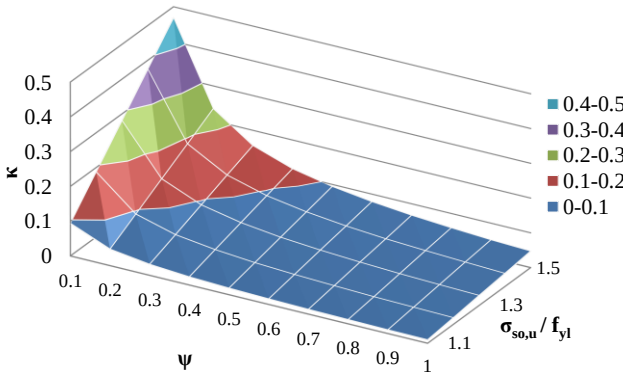

Figure 7: Range of values of κ for typical values of ψ and $\sigma_{so,u}/f_{yl}$

CONCLUSIONS

Strain penetration of the longitudinal reinforcement of reinforced concrete (RC) beams and columns in the joints and/or footings results in fixed-end rotations at the member ends. Accurate determination of these fixed-end rotations at yielding and ultimate limit states becomes of primary importance for defining their inelastic structural response.

Fixed-end rotations are either calculated by over-simplifying empirical approaches that are not able to capture all aspects of strain penetration response or by advanced numerical solutions that cannot be used in everyday engineering practice.

To bridge this gap, this study proposes new closed-form relationships for determining strain penetration fixed-end rotations at yielding and ultimate limit states. The relationships are based on simple yet rational mechanical models that guarantee the accuracy and validity of the results.

REFERENCES

Alsiwat J, Saatcioglu M (1992) "Reinforcement anchorage slip under monotonic loading," *Journal of Structural Engineering*, 118(9):2421-2438

Biskinis DE (2007) Resistance and deformation capacity of concrete members with or without retrofitting, Doctoral Thesis, University of Patras, Greece.

CEB (1993) CEB-FIP Model Code 1990, Bull d' Inf. CEB, 213/214, Laussane, Switzerland

CEN (2005) Eurocode 8: Design provisions of structures for earthquake resistance - Part 3: Assessment and retrofitting of buildings (EN1998-3), Brussels

Fardis MN (2009) Seismic design, assessment and retrofitting of concrete buildings, Springer

Filippou F (1985) A simple model for reinforcing bar anchorages under cyclic excitations, Rep. EERC-85/05, Univ. of California, Berkeley

Lehman D, Moehle JP (1998), Seismic performance of well confined concrete bridge columns, PEER Report 1998/01, Univ. of California, Berkeley

Lowes L, Altoontash A (2003) "Modelling reinforced concrete beam-column joints subjected to seismic loading," *Journal of Structural Engineering*, 129(12):1686-1697

Ma SM, Bertero VV, Popov EP (1976) Experimental and analytical studies on hysteretic behaviour of R/C rectangular and T-beam, Report EERC 76-2, University of California, Berkeley

Mergos PE, Kappos AJ (2012) "A gradual spread inelasticity model for R/C beam-columns accounting for flexure, shear and anchorage slip," *Engineering Structures*, 44:94-106

Otani S, Sozen M (1972) Behavior of multistory R/C frames during earthquakes, University of Illinois, Urbana

Priestley MJN, Calvi GM, Kowalsky MJ (2007) Displacement-based seismic design of structures, IUSS Press, Pavia, Italy

Saatcioglu M, Ozcebe G (1989) "Response of reinforced concrete columns to simulated seismic loading," *ACI Structural Journal*, 86(1):3-12

Sezen H, Setzler EJ (2008) "Reinforcement slip in reinforced concrete columns anchorage slip under monotonic loading," *ACI Structural Journal*, 105(3):280-289

Viwathanatepa S, Popov EP, Bertero VV (1979) Seismic behaviour of reinforced concrete interior beam-column sub-assemblages, Rep. EERC-79/14, Univ. of California Berkeley